A. Al Aboud, E. Dörsam and D. Spiehl – J. Print Media Technol. Res. 9(2020)2, 81–93

81

Investigation of printing pad geometry by using FEM simulation

Ahmad Al Aboud, Edgar Dörsam and Dieter Spiehl

Technische Universität Darmstadt,
Institute of Printing Science and Technology,
Magdalenenstr. 2, 64289 Darmstadt, Germany

aboud@idd.tu-darmstadt.de
doersam@idd.tu-darmstadt.de
spiehl@idd.tu-darmstadt.de

Abstract

Pad printing is an indirect gravure printing for printing on objects with complicated geometries or rough surfaces. Although pad printing is a proven and widely used printing process, there are few scientific studies on the shape and hardness of printing pads and their influence on printing quality. The shape and hardness of printing pads are therefore still determined today by experience. Even in the age of digitalization, the manufacturing of printing pads is still a manual process. So far, no modern tools are known to support this manufacturing process. In this paper, using simulations with commercially available finite element method (FEM) software (Abaqus) or open source software (Salome-Meca) as possible development tools for silicone rubber printing pads is investigated. The FEM simulation of this hyperelastic material requires various input parameters such as material model, special material parameters as well as mesh types and sizes. This paper shows how these parameters are determined, which material tests are necessary and how sensitive the simulation result is to these input parameters. Based on the comparison with experimental data, the results show that silicone rubber printing pads with small deformations can be simulated very well with both the commercial FEM software Abaqus and the free open source FEM software Salome-Meca. Mooney–Rivlin or the polynomial material equations are used. Finally, a workflow is shown with which the geometry of a printing pad can be evaluated and optimized.

Keywords: pad printing, pad geometry, silicone rubber, hyperelastic material, mesh

1. Introduction and background

Indirect gravure printing is a printing process in which a pad transfers the ink from an engraved printing form (cliché) to a substrate. In some literature, it is called pad printing (Hahne, 2001; Kipphan, 2001). The indirect gravure printing method has an acceptable accuracy and a resolution of 20 μm to print, e.g., high accuracy electronic devices (Pudas, Hagberg and Leppävuori, 2004).

Figure 1: Examples of products printed with pad printing; photo from Hakimi Tehrani (2018)

One of the main advantages of pad printing is that it can be used to print on three-dimensional surfaces and products of all shapes and sizes. It does not matter whether the articles are curved or have an uneven surface, with this printing process a high-quality print is nevertheless achieved. If we have to print fine motifs, we will find that the resolution of pad printing is much better than that of screen printing (Tampo Canada, 2018). Figure 1 shows printed examples made by pad printing technology.

The printing pads are made of a liquid mixture of silicone rubber and silicone oil. The shape of the printing pad should be suitable for the substrate to be printed on. This is why there are countless different qualities, sizes, shapes and hardnesses of printing pads on the market. The mixing ratio of silicone rubber and silicone oil determines the surface free energy and the surface hardness of the printing pad, measured in Shore A. Hardnesses from 0 Shore A (soft) to 18 Shore A (very hard) are common. The print quality varies depending on the shape of the substrate to be printed, the printing

pad and its hardness (Al Aboud, et al., 2018). For almost every special printing task it is possible to produce a suitable printing pad to optimize the printing result. Therefore, every manufacturer of printing pads should have several hundred different printing pads on offer (Kipphan, 2001). Today, the choice of printing pad form and hardness is based completely on the expert knowledge of those involved.

In this study the material of the printing pad is described as hyperelastic material. Hyperelastic materials have a clearly different mechanical behavior than, for example, metals, which are also called linear elastic materials. The differences between hyperelastic and linear elastic materials are summarized in Table 1. A more detailed description with explanations can be found in Antman (2004).

Table 1: Difference between hyperelastic and linear elastic material; where σ is tensile stress, E is Young's modulus, ε is extensional strain

Linear elastic material (metal)	Hyperelastic material (printing pad)
$\sigma = E \cdot \varepsilon$ Simple linear relationship between stress and strain.	$\sigma \neq E \cdot \varepsilon$ Complex mathematical equations are used (see section 2).
Very large forces of 9.9 kN to 29.9 kN (1 to 3 tons) cause small deformations.	Small forces of 40 N to 350 N cause large deformations.
Take on a permanently deformed shape after unloading from the plastic deformation.	The material returns to the original form after unloading.
Hardness is measured in Vickers (HV) or Rockwell (HR).	Hardness is measured in Shore A.

In previous investigation, a finite element method (FEM) simulation validation of a printing pad was shown (Al Aboud, et al., 2018). This research concentrates on the sensitivity analysis of the FEM simulation results using the example of a given printing pad made of silicone rubber with 6 Shore A hardness. This 6 Shore A hardness is a medium hardness for printing pads. In order to obtain test specimens with the same specifications (Shore A hardness, material and mixing ratio) as the printing pads, the company Tampo-Technik GmbH was commissioned to manufacture the test specimens and the printing pads.

As shown in (Al Aboud, et al., 2018), the FEM can be a method to study printing pad shapes and loads. The FEM is a numerical method for solving technical problems by calculating the mechanical equation of a real technical operation on the computer. Typical problems solved by FEM are structural analysis, heat transfer,

fluid flow, and acoustics (Shih, 2014). Abaqus (Dassault Systèmes Simulia, 2011) is a very comprehensive FEM program, which has already been used in many studies and simulations (Jungh, et al., 2017). It is a very powerful, but also complex software that requires experienced engineers for modeling. Because of the high licensing costs, it is usually used in large companies or specialized engineering offices. Our approach is to first use Abaqus to investigate the influence of material equations (material model), mesh types, and sizes on the reaction forces. For this investigation, a printing pad with a simple rectangular shape on a flat surface was used, which makes validation very easy (Velten, 2009). For validation, we compared the measured reaction forces on this planar surface of the printing pad from the experiment with the simulated reaction forces from the Abaqus simulation. In a second step, we then used the open source simulation software Salome-Meca and compared the simulation results with the results from Abaqus.

The parameters of the material to be investigated are required for the FEM simulation. For many standard materials these parameters are already available in the FEM software. However, the material properties of silicone rubber printing pads, a hyperelastic material, are unknown. Abaqus can calculate the material constants for the complex behavior of silicone rubber based on the three standardized material characterization methods. These methods are described in the section 2.

2. Determination of mechanical properties

As stated above, printing pads are made of silicone rubber, which is mixed with silicone oil to get a suitable Shore A hardness; that mixture is a kind of an elastomer (Rinnbauer, Stein and Pererseim, 2008). This type of mixing gives the printing pad different mechanical properties, including hardness. Besides the known value of Shore A hardness of the material, it is necessary to determine also the other mechanical properties of silicone rubber to solve the equations of the material deformation. The mechanical properties of this printing pad material should be determined by the Poisson test, volumetric compression test and mechanical tests. Therefore, we have characterized various silicone rubber samples in a Zwick Z050 test machine to obtain the following results.

Poisson's ratio is defined by the ratio of strain in "passive" direction (normal to load) to the "active" strain in length direction (ASTM International, 2014). The Poisson's ratio is calculated according to Equation [1]. The strain in transverse and axial directions is measured with a video extensometer system during the uniaxial tensile test execution at the same time. The value

A. Al Aboud, E. Dörsam and D. Spiehl – J. Print Media Technol. Res. 9(2020)2, 81–93

83

of 0.49 was calculated for silicone rubber test specimens with hardness of 6 Shore A.

$$\text{Poisson's ratio} = \left| \frac{\text{Strain in transverse}}{\text{Strain in axial}} \right| \qquad [1]$$

The uniaxial tensile, compression and planar tensile tests should be executed to get the stress–strain diagram of the silicone rubber material, which is produced under the same boundary conditions as the printing pad with hardness of 6 Shore A. Here, the Zwick Z050 test machine with ± 2 μm position repetition and 27 nm travel resolution accuracy was used to execute the tests. The uniaxial tensile test was performed according to ASTM D412-98a (ASTM International, 1998) and ISO 37 (International Organization for Standardization, 2005) standards. In this case, the dumb-bell shape test specimen type 1 was selected and the test length of 25 ± 0.25 mm on test specimens was marked. A video extensometer system measured the marked area length changes to calculate the strain values in the test process. Force values were measured during the test execution to calculate the stress. Every specimen was loaded and unloaded three times, and the average load curve was used for the FEM simulation to account for slight deviations between them. Figure 2 shows the specimen.
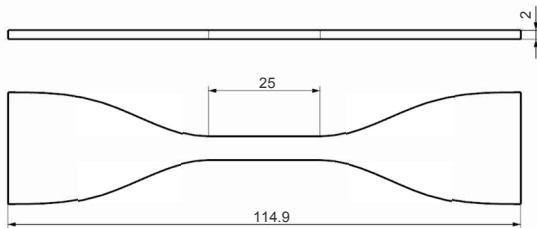

Figure 2: Uniaxial tensile test specimen in accordance to ISO 37 (International Organization for Standardization, 2005), 6 Shore A; size is in mm

The planar tensile test was applied in the same standard till the maximum strain of 55 % with a rectangular test specimen. In this case, the test specimen is a silicone rubber sheet with the test length of 8 mm and width of 60 mm.

The compression test method is defined in ISO 7743 standard (International Organization for Standardization, 2011). The test type B was performed according to this standard on a cylindrical test specimen with diameter of 17.8 ± 0.15 mm and height of 25 ± 0.25 mm.

The experimental results of tensile, planar and compression tests for silicon rubber of 6 Shore A are presented in Figures 3 to 5. The strain and stress loading–unloading behavior of silicone rubber with 6 Shore A hardness are clarified here.
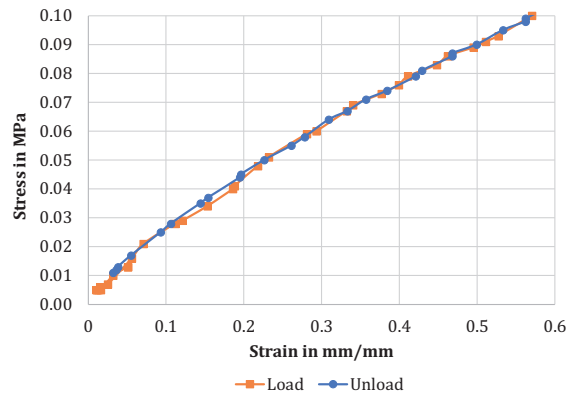

Figure 3: Tensile stress–strain curve (loading–unloading) for 6 Shore A silicone rubber
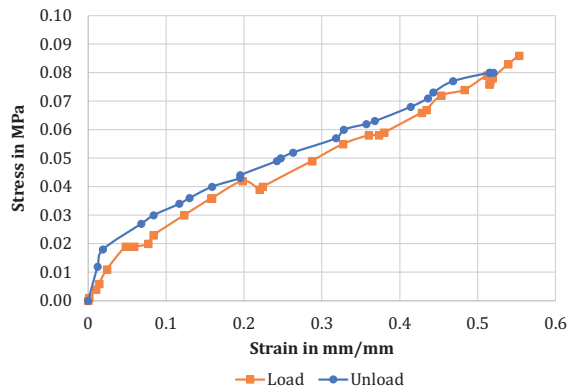

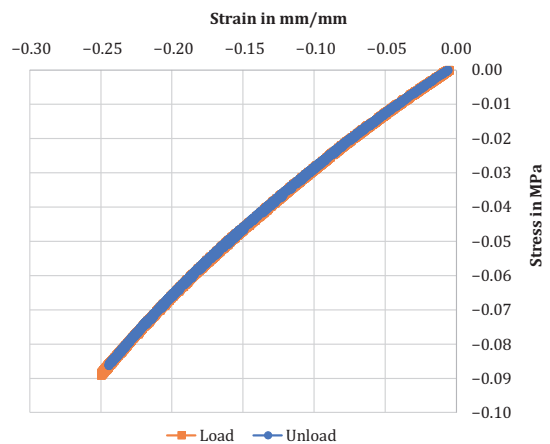*Figure 4: Planar stress–strain curve (loading–unloading) for 6 Shore A silicone rubber*

Figure 5: Compression stress–strain curve (loading–unloading) for 6 Shore A silicone rubber

These data were entered into the FEM software Abaqus as parameters for the printing pad material. Thus, all requirements for a simulation are met, only if the mathematical approximation for the behavior of the silicone material is known. It can be described by

Korochkina, et al., (2008) in a strain energy potential W Equation [2].

$$W(\bar{I}_1, \bar{I}_2, J) = \qquad\qquad\qquad [2]$$
$$\sum_{i+j=1}^{N} C_{ij}(\bar{I}_1 - 3)^i (\bar{I}_2 - 3)^j + \sum_{i=1}^{N} \frac{1}{D_i}(J - 1)^{2i}$$

Where C_{ij} and D_i are material parameters, and J is the elastic volume ratio. These parameters can be obtained by curve fitting to stress–strain data from the mechanical tests (Korochkina, et al., 2008).

For a good engineering approximation, rubber can be considered as incompressible. If the silicone rubber can nevertheless be compressed, a (further) volumetric compression test must be carried out. Equation [2] has only two independent strain invariants, which are $\bar{I}_1$ and $\bar{I}_2$. They are the first and second invariants of the deviatoric left Cauchy-Green deformation tensor (Korochkina, et al., 2008).

If all parameters of Equation [2] are now known via the material tests, then it can be solved by the FEM software. There are several methods for this. Mooney–Rivlin or polynomial equations are mathematical models to define the strain energy equation during deformation of the silicone rubber. They are often used for silicone rubber materials or other hyperelastic materials (Korochkina, et al., 2008). The polynomial equation is selected for all following simulations.

The relation between stress and strain for an incompressible hyperelastic material under tension/compression is elucidated in Equation [3] (Rivlin, 1956)

$$\sigma_e = 2 \cdot (\lambda - \lambda^{-2}) \cdot \left(\frac{\partial W}{\partial I_1} + \frac{1}{\lambda}\frac{\partial W}{\partial I_2}\right) \qquad [3]$$

where σ_e is tension or compression stress, and λ is strain, parallel to σ_e.

Equation 4 shows the relation between stress and strain for an incompressible hyperelastic material under simple shear (Rivlin, 1956).

$$\tau = 2 \cdot \gamma \cdot \left(\frac{\partial W}{\partial I_1} + \frac{\partial W}{\partial I_2}\right) \qquad [4]$$

Where τ ist shear stress, and γ is shear strain.

From stress–strain values of the planar, biaxial test, Poisson test, volumetric compression test and tensile tests the software Abaqus is able to calculate the Mooney–Rivlin or polynomial constants. The calculations are based on a curve fitting method between the measured stress values from experimental tests and the calculated stress from the models for hyperelastic material (Equations [3] and [4]). These constants can also be used later in the open source FEM software Salome-Meca.

3. FEM simulations

We used Abaqus to create an accurate FEM simulation. To approximate the printing pad geometry a three-dimensional mesh is generated by the FEM software. The mesh element type and size play important roles in simulation results (Tadepalli, Erdemir and Cavanagh, 2011). In general, three-dimensional meshes
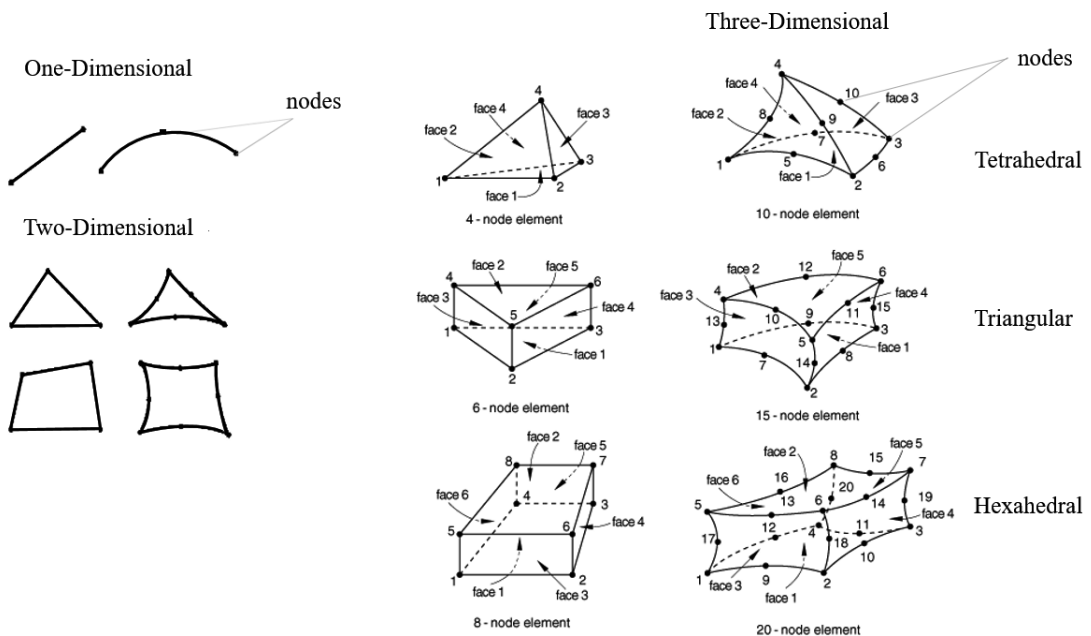

Figure 6: Mesh element types in Abaqus with their nodes, adapted from Dassault Systèmes Simulia (2008)

A. Al Aboud, E. Dörsam and D. Spiehl – J. Print Media Technol. Res. 9(2020)2, 81–93

85

for finite element analysis must consist of tetrahedra, pyramids, prisms or hexahedra. Figure 6 illustrates the mesh types with their nodes. Only three-dimensional mesh types can be used to approximate the pad geometry.

In accordance with the Abaqus manual (Dassault Systèmes Simulia, 2011), the following can be said about the problem at hand: for the given printing pad geometry, only three of the three-dimensional mesh types are possible. These are Tetrahedra (C3D10) with 10 nodes or 4 nodes, Triangular (C3D15) with 15 nodes or 6 nodes and Hexahedra (C3D20) with 20 nodes or 8 nodes. A three-dimensional mesh type is proposed for the mechanical response of two-dimensional heterogeneous materials (Zhang and Katsube, 1995). They are in this simulation silicone rubber (printing pad) against steel (substrate table). Hybrid mesh elements C3D10H are primarily intended for simulating incompressible materials, e.g. hyperelastic behavior modeling with rubber (Dassault Systèmes Simulia, 2011). For the geometry of the silicone rubber printing pads, the mesh element type C3D10MH and C3D10H are used in this simulation, where (M) means the modified mesh element type of C3D10 (Dassault Systèmes Simulia, 2011). In literature (Tadepalli, Erdemir and Cavanagh, 2011) the mesh element type C3D10MH has been used for the simulation of incompressible neo-Hookean material and it has given very good results (Guo, et al., 2016). Reduced integration and modified mesh element types are used in this simulation. This causes buckling of the mesh element with one node. This problem is called hourglassing. In these places of the geometry the mesh density must be increased (Brown, 1997). Table 2 shows the element types used with their properties.

Table 2: Mesh element types used

Mesh element type	Description
C3D10MH	10 nodes, modified mesh element tetrahedron, with hourglass control, hybrid
C3D10H	10 nodes tetrahedron, with hourglass control, hybrid
C3D20H	20 nodes hexahedral, hybrid

The mesh element size is the maximum length of the mesh element in mm. This parameter determines the density of the mesh of the geometry. The mesh element size in this simulation is chosen between 2 mm and 8 mm. Figure 7 shows an example of the mesh with a mesh element size of 5 mm of a printing pad with mesh element type C3D10MH and the flat steel surface with mesh element type C3D20H.
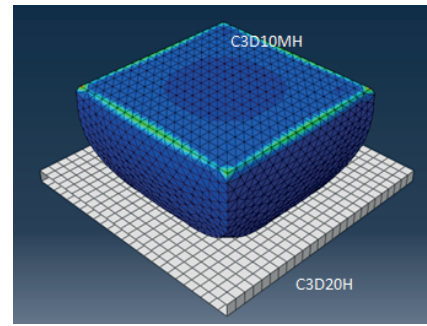

Figure 7: Mesh of a printing pad (74 mm × 72 mm × 52 mm) on a flat steel surface, the mesh element size is 5 mm; mesh element type C3D10MH is used for the printing pad (blue) and mesh element type C3D20H for the flat steel surface

4. Results of the simulation

The Abaqus FEM simulation gives good results close to measured values of displacement (pad deformation path) and the reaction force during printing. The displacement indicates how a small volume element on the printing pad surface shifts due to the deformation caused by the reaction force; the force sensor has a measuring range from 0.1961 N to 980.665 N. The FEM simulation results were validated by means of experimental investigations. An improved pad printing machine (Hakimi Tehrani, Dörsam and Neumann, 2016; Hakimi Tehrani, 2018) is used to monitor the printing pad displacement and reaction force during printing by the use of sensors and it stores the data for analysis. Afterwards, the measured parameters are compared with the simulation results; where in all the diagrams, displacement is the deformation path of the printing pad in the vertical direction on the printing pad base during printing.

Figure 8 illustrates the simulated and measured reaction forces during printing. At the zero point, the top of the pad just touches the flat steel surface. With increasing vertical movement, the reaction forces increase. They do not increase linearly. Figure 8 shows a little difference between the experimental data and the result of simulation of the different mesh elements sizes. This difference is acceptable because the simulation results usually are not exactly matching the experimental results (Tadepalli, Erdemir and Cavanagh, 2011). The simulation results of three different mesh sizes (2 mm, 4 mm, 8 mm) clarify the effect of the size on the simulation results. We can note that the simulation took a very long time for 2 mm elements (about 12 hours) while other sizes 4 mm and 8 mm had nearby the same result with far less time of about 20 minutes. So, we can say that the mesh sizes in this range do not play a significant role in improving the simulation result in this case.
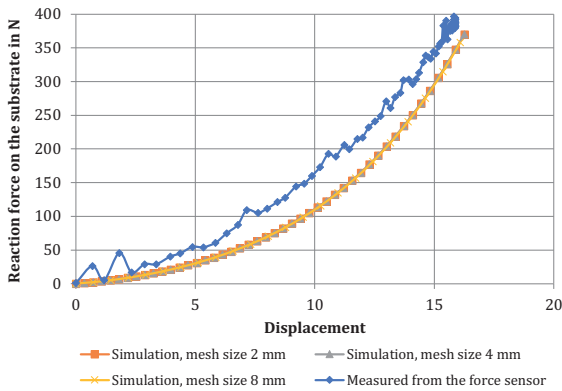
Figure 8: Comparison of the force–displacement diagram from experimental data and the simulation results obtained with Abaqus with three different mesh element sizes

Figure 9 shows the simulation results of different mesh element types with the mesh element size of 4 mm. The mesh element type of C3D10H is compared with C3D10MH. The mesh element type 3D10MH is a modified formulated meshing method (see Table 2). Both mesh element types are compared with the experimental results.
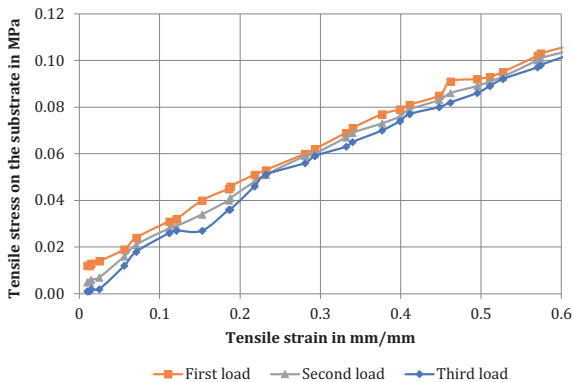

Figure 9: Comparison of the force–displacement diagram from the machine and the Abaqus simulation results with two different mesh element types C3D10H and C3D10MH

Figure 9 shows that the mesh element type C3D10MH does not lead to any improvements. The Abaqus simulation results of both mesh types are identical. It can be concluded that the mesh element type does not play an effective role in the accuracy of the simulation results in this application.

5. Sensitivity analysis of FEM simulation

As mentioned before, the force values from the simulation and the measurement do not match exactly. Small difference between the experimental data and the cal-

culated data depends on the simulation parameters, especially, the material parameters. In the following, a sensitivity analysis is performed to determine the influence of the parameters.

Sensitivity analysis is a method for estimating the range of variation of the results by varying the simulation input variables. In this paper, the input variables are the mechanical properties of the printing pad material and the mathematical models of the hyperelastic material. The sensitivity analysis deals with the assumption: if the simulation results remain stable even with changed input variables, it can be determined how the target function value changes with the variation of input variables and which input variables have what influence on the resulting target function values (reaction force on the substrate during printing) (Schwenk, 2007).

The sensitivity analysis is performed by changing the simulation parameters of the FEM simulation, or by changing the material properties to improve the validation of the FEM simulation. Important input variables are the measured values of the test for characterization of the material by the uniaxial and planar tensile tests and the compression test (see section 2). These tests are performed several times for statistical purposes. In the following we will consider the sensitivity of the simulation in Abaqus from three individually performed tests. Finally, we will investigate the influence of the chosen mathematical model on the accuracy of the Abaqus simulation.

5.1 Effect of the error in the uniaxial and the planar tensile test

The uniaxial and the planar tensile test are considered in this study for the investigation of the error influence by the determination of the material characteristic values.
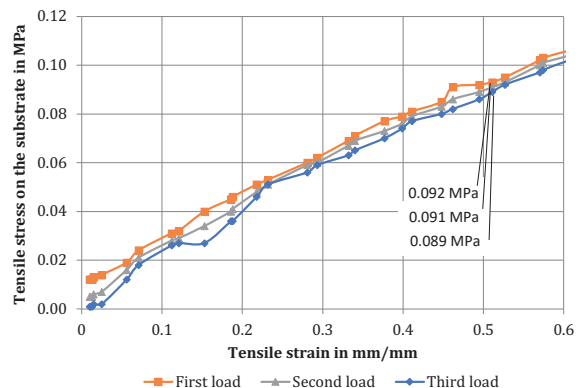

Figure 10: The uniaxial tensile test for one specimen made from 6 Shore A silicone rubber stressed in three cycles, only the load is taken from each cycle

The tensile test was carried out three times on the same tensile specimen with 6 Shore A hardness, and produced three fluctuating datasets. Figure 10 shows the stress–strain diagram for the first, second and third load applied on the tensile specimen.

The datasets are used as input parameters for three Abaqus FEM simulations and thus give three different results for the reaction force. These are shown in Figure 11. A slight divergence can be noticed between the three curves. Figure 11 shows the increased reaction force by increasing the deformation of the printing pad from the simulations.
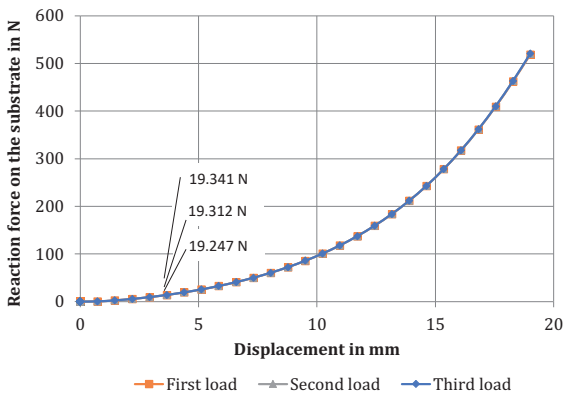

Figure 11: Abaqus simulation results based on the three tensile tests shown in Figure 10, reaction force over the deformation path (displacement) on the printing pad; the mesh element type is C3D10H and the mesh size is 2 mm; the first, second and third simulation is based on the first, second and third tensile stress measurement, respectively

To sum this up, an increase in tensile stress from 0.089 MPa to 0.092 MPa at a strain of 0.5 mm/mm leads to a difference in reaction forces of about 0.1 N at a deformation of 4.3 mm. So, the influence of the tensile test result is very small (see Figures 10 and 11).
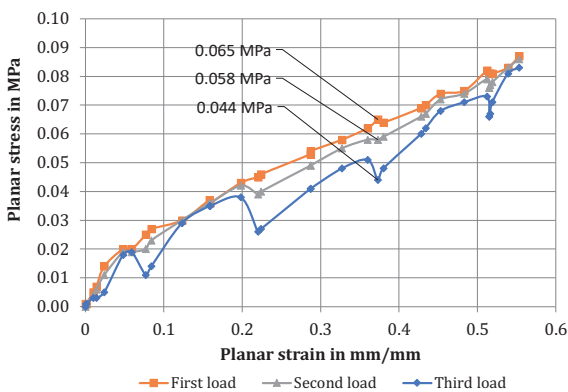

Figure 12: The planar tensile test for one specimen made from 6 Shore A silicone rubber stressed in three cycles, only the load is taken from each cycle
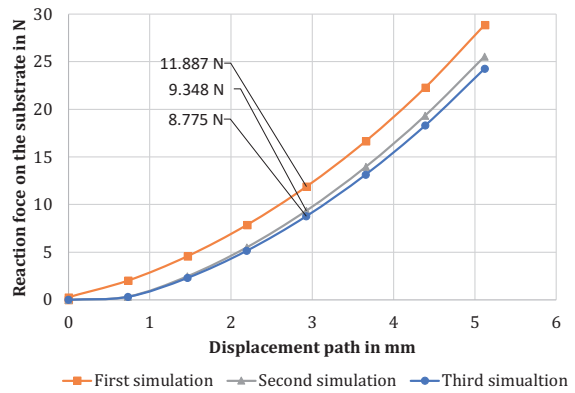

Figure 13: Abaqus simulation results for the three planar tensile tests, reaction force over the deformation path on the printing pad, the mesh element type is C3D10H and the mesh size is 2 mm; the first, second and third simulation is based on the first, second and third planar stress measurement

Let us now look in a similar way at the planar tensile test. The planar specimen is loaded three times. As Figure 12 shows, the fluctuations of the measured values between the individual loads are much bigger than in Figure 10. Somewhat unexpectedly Figure 13 shows that the deviations between the individual loads do not seem as large as the variations in Figure 12 might suggest.

To sum this up, an increase in tensile planar stress from 0.044 MPa to 0.065 MPa at a strain of 0.37 mm/mm leads to a difference in reaction forces of about 3.1 N at a deformation of 2.9 mm. So, the influence of the planar tensile test result is not small. The deviation of the reaction force at a deformation of 2.9 mm is 35.6 % (see Figures 12 and 13).

Nevertheless, the deviations of the different loads in Figure 13 are of great importance for the simulation. The errors in the planar tensile test change the calculated Mooney–Rivlin constants or the calculated polynomial constants, and these change the properties of matter in the simulation. As explained in section 2, these equations define the hyperelastic material for the FEM software. Let us first look at the behavior in compressibility for further understanding.

5.2 Effect of the volumetric compression test

Silicone rubber is normally considered to be incompressible. This is equivalent to a Poisson's ratio of 0.5. Since the determination of the Poisson's ratio is complex, the volumetric compression tests have been used, to provide a dataset of silicone rubber material compressibility.

This test differs from the normal compression test in that the strain on the specimen in this test is a volumetric strain and not a longitudinal strain. We get from volumetric compression test the bulk modulus B.

In volumetric compression test, a cylindrical specimen is pressed into a closed cylinder while the values of the volume change and the associated compression stress is measured. Figure 14 shows the changes in volume ΔV in relation to the total volume due to pressure. The slope of the compression curve is a measure of compressibility and can be described with the bulk modulus. The bulk modulus B is calculated with the Equation [5] (Brotzman and Eichinger, 1982):

$$B = \frac{\Delta P}{\Delta V / V} \qquad [5]$$

Where ΔP is the pressure difference between two points on the curve in Figure 14. The calculated bulk modulus is 500 MPa and the material is, therefore, incompressible.

In Salome-Meca the bulk modulus is calculated from the Poisson's ratio and the constants in the Mooney–Rivlin equation using Equation [6]:

$$B = 2 \cdot (C01 + C10)/(1 - 2 \cdot v) \qquad [6]$$

where C01 and C10 are Mooney–Rivlin constants and v is the Poisson ratio (Gehrmann, et al., 2017).
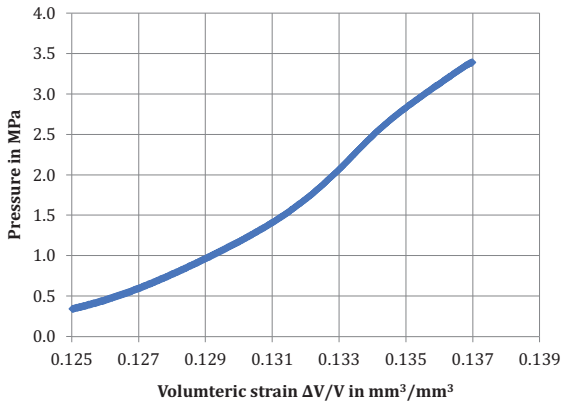

Figure 14: The measured results of the volumetric compression test; the volumetric change ΔV as a result of the pressure in relation to the total volume V is plotted

Moreover, the influence of the volumetric compression test on the simulation results is relatively small, as shown in Figure 15. In the next step, the datasets of the volumetric compression tests are compared with the theoretical data using a Poisson's ratio of 0.5. The Abaqus simulation results are shown in Figure 15. There is no difference between the simulation results based on the data from the volumetric compression

test and the theoretical values with a Poisson's ratio of 0.5. For our study the low compressibility of the printing pad material can therefore be ignored in the simulation. However, it can also be observed that the simulated deformations deviate from the measured values and are always larger at the same force.
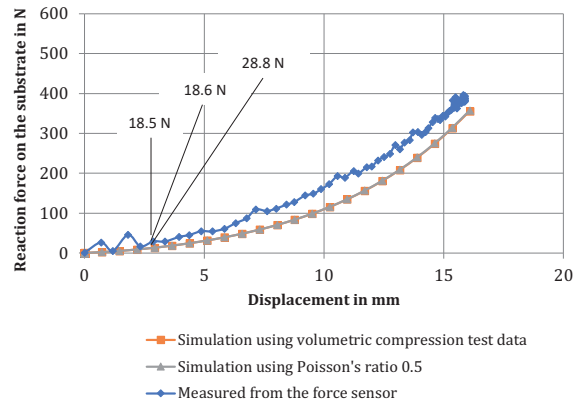

Figure 15: Comparison of resultant reaction forces versus displacement using the compression test and Abaqus simulation (mesh element type is C3D10H and the mesh size is 2 mm) for a Poisson's ratio of 0.5 and for using the data from the compression test; a measurement is shown for comparison

To sum this up, the use of measurement results from the volumetric compression test in the simulation leads to a small increase of the reaction force at a deformation of 2.9 mm by 0.1 N. The simulation results of both simulations are almost identical. However, the simulated deformations deviate from the measured values and are always greater with the same force (see Figure 15).

5.3 Effect of the biaxial test

From the data of the compression test and the other previous tests (see Figure 5), Abaqus can calculate the Mooney–Rivlin or polynomial constants for the material. Therefore, the compression test is usually performed. The uniaxial compression stress and biaxial stress are considered in small deformations equal (Hakimi Tehrani, 2018). The uniaxial compression test setup is simple and it can be performed quickly (see section 2). With hyperelastic materials, however, the calculation of the constants becomes often much more accurate when another test is done, the so called biaxial tensile test. This test is much more complex than the compression test. However, it has the advantage that the achievable strains are less limited.

The biaxial tensile test is similar to the uniaxial tensile test. However, the specimen is drawn simultaneously in two spatial directions. A cross-shaped flat specimen is loaded on four sides. This test requires a special test bench with

complex measuring technology (Seibert, Scheffer and Diebels, 2014). Therefore, it should always be considered whether the biaxial tensile test is really needed.

Without conducting the biaxial tensile test, we would like to make some considerations for the usefulness of the test. For this we used the results of the compression test from Figure 5 (see section 2). Here we see that the simulation results (reaction force on the substrate with displacement) differ from the measured values from the force sensor (see Figure 16). We therefore want to look into the question of which influence the measured data have on the determination of the Mooney–Rivlin or polynomial constants. If the measured compression stress values are multiplied by a constant factor, the specimen shows a stiffer behavior. For further consideration the compression stress values of Figure 5 were multiplied by 1.5 and entered as input parameters in the Abaqus simulation. The results are given in Figure 16. The graph for the compression test from Figure 5 and the measured values of the reaction force from Figure 16 are shown. Furthermore, the Abaqus simulation results are plotted with the multiplied values (modified compression test values). To our surprise these simulated values correspond very well with the measured values from Figure 5 up to a deformation of 10 mm. This means that with a stiffer material the behavior of the printing pads can be described much better. A better description of the material can be achieved by determining the constants more precisely. This is made possible by a biaxial tensile test. For further investigations, the biaxial tensile test should therefore be carried out for the simulation of silicone rubber printing pads. For deformations up to 10 mm we could also use the results from the modified compression test (see Figure 16) as a first approximation.
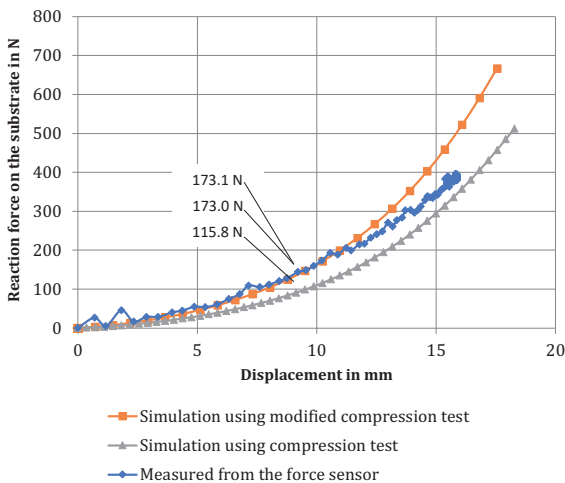

Figure 16: Abaqus simulation (mesh element type is C3D10H and the mesh size is 2 mm) using data from the compression test and from a modified compression test compared to experimental data

To sum this up, the deviation of the reaction force at a deformation of 9 mm is 0.05 % for the simulation with modified compression test and 33 % for the simulation with compression test (see Figure 16).

To get more effective results, we developed the biaxial clamps to fit the available Zwick Z050 test machine and silicone rubber material, and use this results in the simulation. The experimental result of biaxial tensile test for silicon rubber of 6 Shore A is presented in Figure 17.
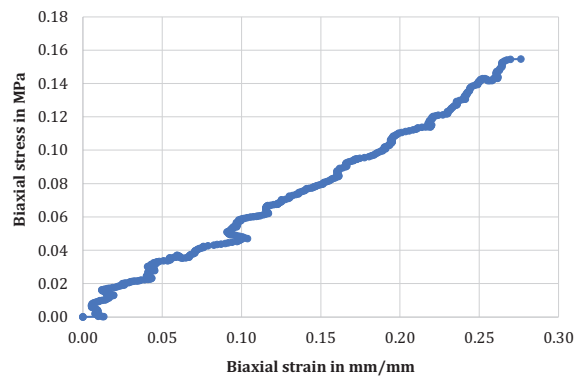

Figure 17: Measured results of the biaxial tensile test for 6 Shore A silicone rubber

By comparing the absolute results in Figure 17 with Figure 5 at strain 0.25, we get 1.5 times more stress at the same point in Figure 5.
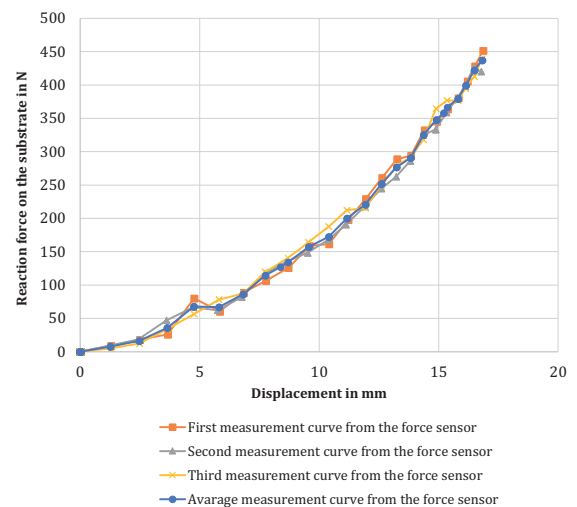

Figure 18: Measured results of the force sensor

After that, we performed three measurements on the force sensor to confirm previous measurements result and took the average curve, in consideration that all measurements begin at the touching point between the printing pad surface and the substrate, which is 145 mm on the servo motor (0 mm displacement), and

90

A. Al Aboud, E. Dörsam and D. Spiehl – J. Print Media Technol. Res. 9(2020)2, 81–93

keep servo motor going on until 162 mm (17 mm displacement), see Figure 18.

Finally, we compare simulation using biaxial test and simulation using compression test with average measurement curve from the force sensor, to find that our simulation using biaxial test is more reliable and effective (see Figure 19).
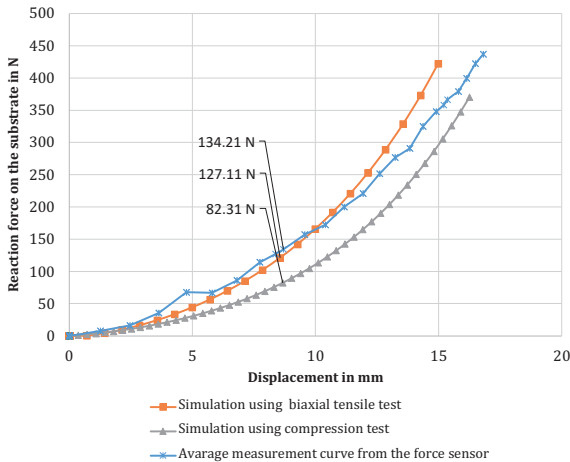

Figure 19: Abaqus simulation (mesh element type is C3D10H and the mesh size is 2 mm) using data from the compression test and from biaxial tensile test compared to average measurement curve from the force sensor

In summary, it can be said that the deviation of the reaction force at a deformation of 8.5 mm is 5 % in the simulation with biaxial tensile test and 34 % in the simulation with compression test (see Figure 19). The use of the biaxial tensile test therefore leads to a better simulation result of printing pads.

5.4 Effect of the mathematical model

The behavior of the deformed material is described by material models (equations); these models are the basis for every FEM simulation. As already explained in section 2, the polynomial equation is selected for all previous simulations. There are many mathematical models to describe the material behavior of silicone rubber. In the following, three simulations with three different mathematical models are carried out. These models are Mooney–Rivlin, polynomial and neo-Hooke (see section 2).

Figure 20 shows the reaction force over the deformation path for the three simulations and the experimental data resultant from the force sensor. As shown in Figure 20, the neo-Hooke simulation does not fit the experimental data at all. This shows how important the correct selection of equations is. As Figure 20 also shows, the simulation results of the Mooney–Rivlin and polynomial equations for small deformations are

approximately equivalent. For further investigations, the simulation quality can be further improved by better material tests, i.e. in particular by an additional biaxial tensile test.
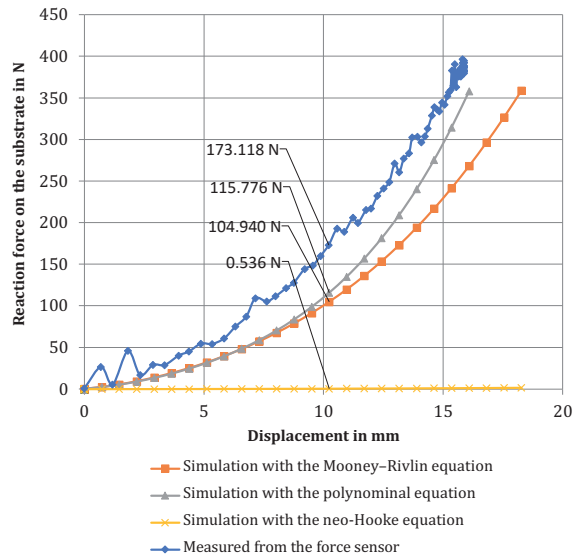

Figure 20: Abaqus simulation (mesh element type is C3D10H and the mesh size is 2 mm) using Mooney–Rivlin equation, polynomial equation and neo-Hooke equation compared to experimental data

The concavity of the resulting curve from polynomial model is very similar to the measured curve from force sensor. When the pad is stiffer, as shown in Figure 16, the two curves are the same.

6. Workflow for improving the printing pad geometry

For small deformations, as they will occur for printing pads, a development tool for the investigation and design of silicone rubber printing pads has been found. In principle it is now possible to investigate and optimize the geometry of a printing pad using FEM simulation. The necessary workflow is shown in Figure 21. For the realization of an FEM based geometry optimization of printing pads already certain basic knowledge in the use of FEM software is recommended.

The first step is to load the geometry of the substrate to be printed in the FEM software and create an FEM model. The FEM model also includes the material data of the silicone rubber, which must be determined beforehand with the described material tests (see section 2). Furthermore, it is recommended to use either the polynomial or Mooney–Rivlin equations. In the second step, the user has to select a pad geometry, which should be optimized, and start the FEM simula-

tion. Based on the calculated results, the user can then decide whether the results meet the requirements or whether a different or modified printing pad geometry should be simulated. The most important requirement for a good pad geometry is the zero displacement on the printing surface of the printing pad. The second requirement is to keep the internal pressure low, because very high pressures lead to permanent deformation of the pad material after a period of time. After going through several iterations, the printing pad geometry can be determined with the desired requirements.
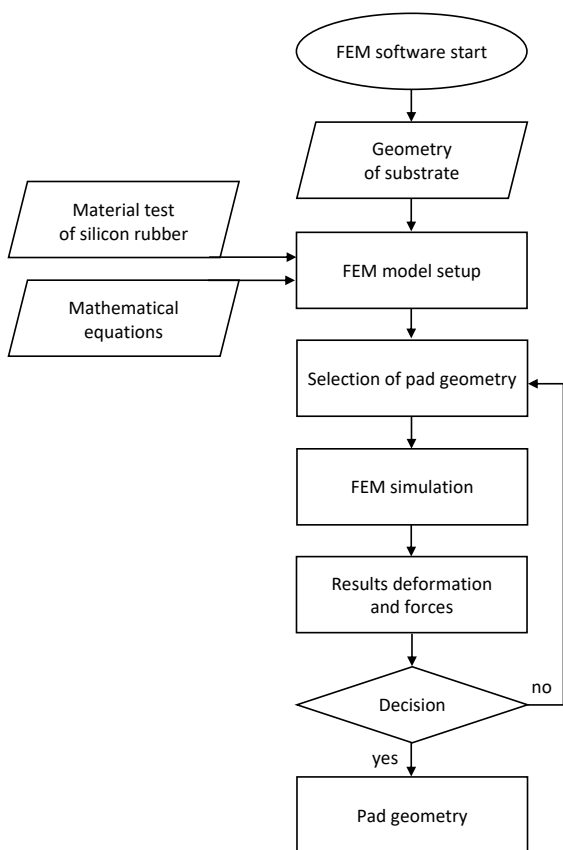

Figure 21: Workflow for investigation of printing pad geometry by using FEM simulation

It should be noted that the geometry of the printing pad cannot yet be calculated automatically with this workflow. The pad printing process is too complex for this. In the future, however, further investigations will lead to the step-by-step development of further tools.

7. Comparison of Abaqus and Salome-Meca software

As mentioned before, printing pad manufacturers are often rather small companies and therefore cannot afford the high license fees of Abaqus. Therefore, a first study will be conducted to check whether the open

source FEM software Salome-Meca is also suitable for a simulation of printing pads. The FEM software Salome-Meca can also simulate hyperelastic materials using polynomial and Mooney–Rivlin equations. Similar to Figure 20, the reaction force on the substrate was therefore simulated as a function of the displacement (deformation path of the pad) and compared with the measured values.
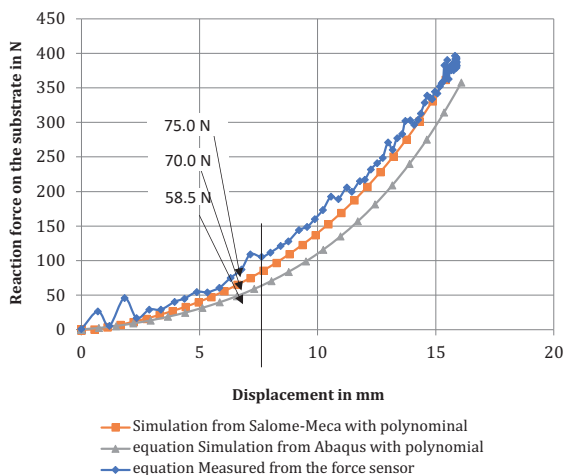

Figure 22: Abaqus and Salome-Meca simulations with polynomial equations compared to measured data

Figure 22 shows the measured reaction forces and the simulation by Abaqus and Salome-Meca. In both simulations the polynomial equation was used. The constants of the polynomial equation were calculated from the material tests with Abaqus software to use these constants in Salome-Meca software. The open source software Salome-Meca achieves good results. The graph is much closer to the measured values than the results of Abaqus. This is especially important for the expected small deformations of printing pads. The difference in Salome-Meca from Abaqus is that Salome-Meca calculates the bulk modulus from the constants of Mooney–Rivlin equation and Poisson's ratio.

From the Abaqus and Salome-Meca simulations we can plot the displacement field in *x* direction and *z* direction of the surface of the printing pad.

Figure 23 shows that the results from both software are very similar and in the center of the printing pad the displacement is at its lowest. It is recommended to place the print image as close as possible to the center of the printing pad. With this type of graphics, a user can see whether the allowed deformation in a particular, interesting area of a layout is met or exceeded.

If the displacement during the printing process is known from the simulation, we can learn more about the deformation of the print image in any direction.

The precision of printing sharp edges in pad printing is a problem due to the expandability of the pad surface. This makes it difficult for printing of microelectronics (Bodenstein, et al., 2019). The shape of the printing pad can be developed in such a way that we achieve the smallest possible deformation of the surface of the printing pad.

Mesh–model from Abaqus   *Mesh–model from Salome-Meca*

Displacement field in x-direction in mm from Abaqus   *Displacement field in x-direction in m from Salome-Meca*

Displacement field in z-direction in mm from Abaqus   *Displacement field in z-direction in m from Salome-Meca*
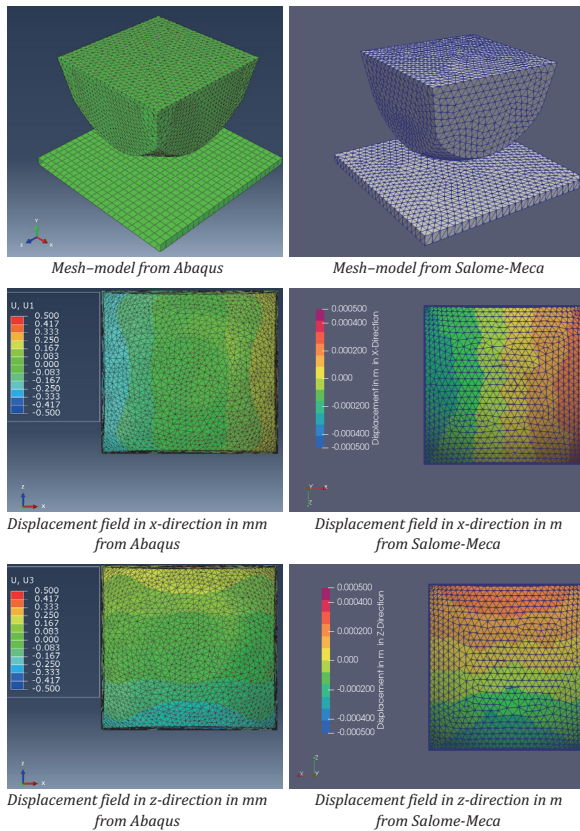
Figure 23: Comparison between simulation results from Abaqus and Salome-Meca of the same printing pad (74 mm × 72 mm × 52 mm) on a flat steel surface at a displacement of 3 mm, the mesh element size is 4 mm, and Mesh element type C3D10MH (please note that the results from Abaqus are plotted in mm and that of Salome-Meca in m)

The differences between the FEM software Abaqus and Salome-Meca have been clarified. However, it is pleasing to note that the free open source software Salome-Meca is basically suitable for the optimization of silicone rubber printing pads.

8. Conclusion and outlook

Even in the age of digitalization, the manufacturing of printing pads is still a manual process. So far, no modern tools are known to support this manufacturing process. In this paper we focus on how FEM software can be used to optimize the geometry of a silicone rubber printing pad. Silicone rubber is a polymeric, elastic material, whose data are not available in the usual FEM programs. Therefore, uniaxial tensile, planar tensile and compression tests have to be performed. After all, suitable equations have to be found for the FEM model setup.

In this study, investigations were performed with the FEM software Abaqus and the Mooney–Rivlin and polynomial constants were determined. The simulation results for a given printing pad were compared with measured deformations and forces. A comparison shows deviations, especially for larger deformations. A sensitivity analysis shows that an additional biaxial tensile test is a possibility to determine the material properties more accurately. The results also show that a simulation is well possible for small deformations. A workflow is shown how a geometry of a printing pad can be simulated and optimized. Finally, it is shown that the open source FEM software Salome-Meca can be used to simulate and optimize silicone rubber printing pads.

This study is an introduction to modern development tools for the design of printing pads. Basically, the FEM method is suitable to support the design and optimization of printing pads. Nevertheless, some open questions remain, which should be clarified in further investigations. For example, the biaxial tensile test should be validated in addition to the characterization of the materials. Thus, the Mooney–Rivlin and polynomial constants can be determined more precisely and the deviations from experimental data can be reduced. The surprising differences between the Abacus and Salome-Meca simulations should also be investigated.

References

Al Aboud, A., Dörsam, E., Hakimi Tehrani, A. and Spiehl, D., 2018. Using FEM simulation as a tool to develop pad printing. In: P. Gane, ed. *Advances in Printing and Media Technology: Proceedings of the 45th International Research Conference of iarigai*. Warsaw, Poland, October 2018. Darmstadt, Germany: iarigai.

Antman, S.S. ed., 2004. *The non-linear field theories of mechanics*. 3rd ed. Berlin, Heidelberg, Germany: Springer.

ASTM International, 1998. *ASTM D412-98a Standard test methods for vulcanized rubber and thermoplastic rubbers and thermoplastic elastomers-tension.* West Conshohocken, PA, USA: ASTM International.

ASTM International, 2014. *ASTM D638-14 Standard test method for tensile properties of plastics.* West Conshohocken, PA, USA: ASTM International.

Brown, J., 1997. Characterization of MSC/NASTRAN & MSC/ABAQUS elements for turbine engine blade frequency analysis. In: *MSC Aerospace Users' Conference Proceedings*. Newport Beach, CA, USA, 17–20 November 1997.

Brotzman, R.W. and Eichinger, B.E., 1982. Volume dependence of the elastic equation of state. 3. Bulk-cured poly (dimethylsiloxane)*. Macromolecules*, 15(2), pp. 531–535. https://doi.org/10.1021/ma00230a061.

Bodenstein, C., Sauer, H.M., Fernandes, F. and Dörsam, E., 2019. Assessing and improving edge roughness in pad-printing by using outlines in a one-step exposure process for the printing form. *Journal of Print and Media Technology Research*, 8(1), pp. 19–27. https://doi.org/10.14622/JPMTR-1903.

Gehrmann, O., Kröger, N.H., Erren, P. and Juhre, D., 2017. Estimation of the compression modulus of a technical rubber via cyclic volumetric compression tests. *Technische Mechanik*. 37(1), pp. 28–36. https://doi.org/10.24352/UB.OVGU-2017-048.

Guo, Z., Chen, Y., Peng, X., Shi, X., Li, H. and Chen, Y., 2016. Shear stiffness of neo-Hookean materials with spherical voids*. Composite Structures*, 150, pp. 21–27. https://doi.org/10.1016/j.compstruct.2016.04.046.

Hakimi Tehrani, A., Dörsam, E. and Neumann, J., 2016. Improving automation and process control of an indirect gravure (pad) printing machine. *Acta Polytechnica Hungarica*, 13(4), pp. 221–240. https://doi.org/10.12700/APH.13.4.2016.4.14.

Hakimi Tehrani, A., 2018. *Automation improvement of indirect gravure printing with a focus on the mechanical characteristics of silicone rubber pads.* Dr.-Ing. Dissertation. Technische Universität Darmstadt.

Hahne, P., 2001. *Innovative Drucktechnologien: Siebdruck-Tampondruck..* Lübeck, Germany: Verlag Der Siebdruck.

International Organization for Standardization, 2005. *ISO 37:2005 Rubber, vulcanized or thermoplastic – Determination of tensile stress–strain properties*. Geneva, Switzerland: ISO.

International Organization for Standardization, 2011. *ISO 7743:2011 Rubber, vulcanized or thermoplastic – Determination of compression stress–strain properties.* Geneva, Switzerland: ISO.

Jungh, T., Glasenapp, T., Fraas, M., Schulz, A. and Bauer, H.-J, 2017. Durchführung von FEM Simulationen zur Anwendung des Superpositionsprinzips der Filmkühlung*. In: *Proceedins of Deutscher Luft- und Raumfahrtkongress 2017*. München, Germany, 5–7 September 2017. Bonn, Germany: Deutsche Gesellschaft für Luft- und Raumfahrt.

Kipphan, H. ed., 2001. *Handbook of print media*. Heidelberg, Germany: Springer.

Korochkina, T.V., Jewell, E.H., Claypole, T.C. and Gethin, D.T., 2008. Experimental and numerical investigation into nonlinear deformation of silicone rubber pads during ink transfer process*. Polymer Testing*, 27(6), pp. 778–791. https://doi.org/10.1016/j.polymertesting.2008.06.003.

Pudas, M., Hagberg, J. and Leppävuori, S., 2004. Printing parameters and ink components affecting ultra-fine-line gravure-offset printing for electronics applications. *Journal of the European Ceramic Society*, 24(10–11), pp. 2943–2950. https://doi.org/10.1016/j.jeurceramsoc.2003.11.011.

Rinnbauer, M., Stein, G., Peterseim, V., 2008. Elastomere. In. H. Domininghaus, P. Elsner, P. Eyerer and T. Hirth, eds. *Kunststoffe: Eigenschaften und Anwendungen*. Berlin, Germany: Springer.

Rivlin, R.S., 1956. Large elastic deformations. In F.R. Eirich, ed. *Rheology*. New York: Academic Press, pp. 351–385.

Schwenk, C., 2007. *FE-Simulation des Schweißverzugs laserstrahlgeschweißter dünner Bleche Sensitivitätsanalyse durch Variation der Werkstoffkennwerte.* Dr.-Ing. Dissertation. Technische Universität Berlin.

Seibert, H., Scheffer, T. and Diebels, S., 2014. Biaxial testing of elastomers: experimental setup, measurement and experimental optimisation of specimen's shape*. Technische Mechanik*, 34(2), pp. 72–89. https://doi.org/10.24352/UB.OVGU-2017-054.

Shih, R., 2014. *Introduction to finite element analysis using SolidWorks simulation.* Klamath Falls, OR, USA: SDC Publications.

Dassault Systèmes Simulia, 2008. *Abaqus analysis user's manual*. [online] Providence. RI, USA: Dassault Systèmes Simulia Corp. Available at: <http://130.149.89.49:2080/v6.8/books/usb/default.htm?startat=pt06ch23s01ael01.html> [Accessed December 2019].

Dassault Systèmes Simulia, 2011. *Abaqus 6.11 theory manual*. [pdf] Providence. RI, USA: Dassault Systèmes Simulia Corp. Available at: <http://130.149.89.49:2080/v6.11/pdf_books/THEORY.pdf> [Accessed December 2019].

Tadepalli, S.C., Erdemir, A. and Cavanagh, P.R., 2011. Comparison of hexahedral and tetrahedral elements in finite element analysis of the foot and footwear. *Journal of Biomechanics*, 44(12), pp. 2337–2343. https://doi.org/10.1016/j.jbiomech.2011.05.006.

Tampo Canada, 2018. *Pad printing vs. screen printing – the differences explained.* Tampo Canada Inc. [online] Available at: <https://www.tampocanada.com/pad-printing-vs-screen-printing> [Accessed December 2019].

Velten, K., 2009. *Mathematical modeling and simulation: introduction for scientists and engineers.* Weinheim, Germany: Wiley-VCH.

Zhang, J. and Katsube, N., 1995. A hybrid finite element method for heterogeneous materials with randomly dispersed rigid inclusions. *International Journal for Numerical Methods in Engineering*, 38(10), pp. 1635–1653. https://doi.org/10.1002/nme.1620381004.